A new perspective of assessing flood impact with daily nighttime light remote sensing data

Yang Hu[a, *], Dai Yamazaki[b], Xudong Zhou[b,c], Gang Zhao[b,d]

[a] Department of Civil Engineering, Graduate School of Engineering, The University of Tokyo, Tokyo, Japan

[b] Global Hydrological Prediction Center, Institute of Industrial Science, The University of Tokyo, Tokyo, Japan

[c] Institute of Hydraulics and Ocean Engineering, Ningbo University

[d] Department of Transdisciplinary Science and Engineering, Tokyo Institute of Technology, Tokyo, Japan

*Corresponding author:

Yang Hu (ORCID: 0000-0002-3024-8811)

Email: yanghu0724@gmail.com yang.hu@rainbow.iis.u-tokyo.ac.jp

Highlights:

1. Satellite nighttime light (NTL) provides reliable proxies for flood impact severity and duration at a pixel scale, with daily resolution.
2. NTL data can detect flood impacts beyond inundation areas, which has been largely missed by satellite-based inundation.
3. The global-scale analysis revealed spatial variations in NTL flood impact, correlating with local development and flooding severity.

Abstract

Flooding leads to disastrous impacts on human society and activities worldwide, including damage to physical assets and interruptions to daily activities. However, evaluation for such impacts remains challenging, particularly beyond inundation zones, due to the difficulties in monitoring human activities on a global scale. Nighttime light (NTL) remote sensing data provides a unique perspective for human activities on a large scale, reflecting variations in light intensity caused by flood impact. Here we show the possibility of using a high-quality NTL dataset to assess flood impact on human society and activities. Indices providing impact severity and duration were generated with NTL as proxies for flood impact on pixel scale. Results show the consistency of NTL-derived and reported impact duration for five selected cases, which confirms the reliability of NTL flood impact. A large portion (> 96%) of NTL-based affected areas did not overlap with the satellite-based inundation area for 99 cases in 2013, indicating the unique value of NTL in assessing flood impact beyond inundation. The NTL flood impact indices were mapped at 15 arc-second spatial resolution for 876 events on a global scale from 2013 to 2021. Then, administrative-level characteristics of NTL flood impact were compared at a global scale. It was found that lower developed regions exhibit higher vulnerability and challenge in recovery, and are more likely to experience extremely serious and long-lasting impacts compared to higher developed areas. Overall, using NTL data, in addition to conventional inundation-based methods, offers an innovative perspective on flood impact evaluation.

Plain Language Summary

Flooding leads to disastrous impacts on human society and activities worldwide, including physical asset damages, displacement and fatalities, disturbance of industrial and service activities in society. Evaluation for such impacts remains challenging, particularly beyond inundation zones, especially on a global scale. We here explored a new approach using nighttime light (NTL) remote sensing data to assess flood impact globally. Flood impact severity and duration in pixel detail can be estimated with NTL data. Results show the consistency of NTL-derived and the reported impact duration for five selected cases, which confirms the reliability of NTL flood impact. A large portion (> 96%) of NTL-based affected areas did not overlap with the satellite-based inundation area for 99 cases in 2013, indicating the unique value of NTL in detecting flood impact beyond inundation. Flood impact severity and duration were mapped for 876 events that happened from 2013 to 2021 globally and further compared at the administrative level. We discovered that flood impacts vary across regions, with areas of lower development experiencing more severe and longer-lasting impacts. Overall, this research offers a new perspective on evaluating flood impacts globally, which could improve our understanding and management of flooding events.

1. Introduction

Flooding, a significant and recurring natural hazard, exerts a substantial and far-reaching impact on human society and activities. Such impact includes the physical assets damages, displacement and fatalities, disturbance of industrial, service (trade, restaurants, companies etc.), and public (schools, hospitals, churches etc..) sectors in the society (Jonkman et al., 2008; Merz et al., 2010; Smith & Ward, 1998). Flood impact can happen within or beyond inundation areas (Johnmen et al., 2012; Jonkman et al., 2008; Merz et al., 2010; Smith & Ward, 1998). The impact within the inundated area is due to the physical contact with flood water, while the one out of the inundation area is due to a cut of supply (e.g., electricity, production material).

Assessment for flood impact within and beyond inundation areas are equally important for guiding disaster relief and adaptation policies (IPCC, 2012; Jongman et al., 2015; Merz et al., 2010; Taguchi et al., 2022; Tanoue et al., 2020; Tellman et al., 2021; Winsemius et al., 2013). Models and methods have been well developed and employed to estimate flood impact within inundation areas on a global scale. Many global studies considered the hazard, exposure, and vulnerability to estimate the affected GDP, affected population, as well as the physical asset damage by flooding (IPCC, 2012; Jongman et al., 2015; Tellman et al., 2021; Winsemius et al., 2013). Direct economic loss due to industrial and service interruption is estimated by considering the inundation duration and daily production value (Taguchi et al., 2022; Tanoue et al., 2020). These studies give comprehensive evaluations of potential flood impact within the inundation area.

Compared to the flood impact within the inundation area, the one beyond inundation is more difficult to estimate (Merz et al., 2010), and limited studies exist. A computable general equilibrium (CGE) model has been developed and used to estimate the high-order economic loss for all affected areas on a global scale (Ciscar et al., 2011; Dottori et al., 2018; Tanue et al., 2020). However, the model mainly focuses on long term GDP losses on a large-scale (national scale) and needs much auxiliary data input. Hence, the short-term and local-scale impact on human society is still not well explored and evaluated in an efficient and simple way beyond the inundation area. Moreover, studies about flood impact seldom delve into the intricate implications of floods on human daily life, encompassing displacement and disruptions in the public sector (e.g., household power outage, close of school or hospital), particularly on a global scale (Koks et al., 2019). This may lead to an underestimation of flood impact both within and

out of the inundation. The gaps might be attributed to the limited availability of data that reflects human activities and the reactions toward flooding at a large scale.

The nighttime light (NTL) remote sensing data records nocturnal light and provides a unique perspective into human activities and societal dynamics on the global scale (Elvidge et al., 2001, 1997). For instance, NTL data have been widely used in many aspects including revealing the impacts of natural disasters (Elvidge et al., 1997; Li et al., 2022; Wang et al., 2018; Zheng et al., 2022; Zhou et al., 2014). When a flood happens, impacts including damages to residential buildings, displacement and fatalities, interruptions in the industry, manufacturing, service, and public sectors will happen within and beyond the inundation areas. Due to the mentioned reasons, the light intensity of affected human settlements, industrial, commercial, and public areas should be reduced compared to normal status (Enkel et al., 2012). In 2020, the National Aeronautics and Space Administration (NASA) released the global daily Lunar-BRDF corrected NTL dataset of NASA's NPP/VIIRS Black Marble product suite (VNP46A2) with 15 arc-second spatial resolution (Román et al., 2022, 2018). This pioneering product effectively mitigates most uncertainties associated with VIIRS DNB's top-of-atmosphere (TOA) radiance (Román et al., 2018; Wang et al., 2021). Further corrections are needed to exclude remaining errors due to daily observational coverage mismatch and angular effect (Hu et al., 2024). The high-quality, consistent daily NTL product becomes a powerful tool for scrutinizing human activities and responses to short-term events, even within spans of just a few days. Thus, this NTL product can be employed to provide proxies for flood impact both within and beyond inundation areas on human society and activities globally by simply checking the light intensity variation due to flooding.

Some studies have already leveraged NTL data to detect flood-related disaster impacts for specific flood event cases. Enenkel et al. (2020) introduced an innovative strategic framework utilizing NTL information for displacement monitoring. They applied this approach to a real-world case study involving Tropical Cyclone "Idai," which struck Mozambique and led to flooding in March 2019. Wang et al. (2018) focused on monitoring the spatial extent of power outages and recovery status at the community level following Hurricane Sandy, a historic storm that made landfall on the northeastern coast of the United States and triggered flooding in late October 2012. Zhao et al. (2018) evaluated intensity changes before and after a disaster in selected cases, substantiating the utility of daily NTL data in detecting damages, power outages,

and other adverse outcomes stemming from flooding and other disasters. However, these studies predominantly concentrate on individual cases. An analysis of flood impact for historical cases on a global scale is still lacking. Meanwhile, they did not employ preprocess for the daily NTL VNP46A2 product, which might affect the detection of light intensity variation (Hu et al., 2024).

This study aims to employ high quality daily consistent NTL dataset to assess flood impact on human society and activities globally. Our approach involves evaluating the NTL's effectiveness in detecting flood impact through case studies, exploring the potential for event-based monitoring of impacts, and assessing the uniqueness of flood impact information derived from NTL data. The research also encompasses an analysis of flood impact on a global scale over the past decade (2013 – 2021). With the NTL-derived flood impact, we seek to contribute to a deeper understanding of the flood impact on human society and activities on a global scale.

2. Data

The daily Lunar-BRDF corrected NTL of NASA's Black Marble product (VNP46A2) (Roman et al., 2018) with a 15 arc-second (about 500 m) spatial resolution was used in this study. The VNP46A2 dataset has excluded most uncertainties of the at−sensor TOA radiance (VNP46A1). The main process includes lunar irradiance modeling, atmospheric corrections, and BRDF corrections that consider moonlight, aerosols, surface albedo, and seasonal vegetation patterns with globally consistent equations reflecting the physical mechanisms in relevant factors (Román et al., 2018). The dataset contains seven layers, including the daily light intensity and quality control information (Román et al., 2022). We specifically employed the Lunar-BRDF-corrected layer of the VNP46A2 product from 2013 to 2021. The satellite zenith angle layers from the VNP46A1 product were utilized during the data correction process. The cloud mask, quality flag and snow flag layers from VNP46A1 and VNP46A2 products were used to make quality control and obtain definitely clear observations. The Black Marble products are available at the https://blackmarble.gsfc.nasa.gov/#product.

We collected global flooding cases from the Dartmouth Flood Observational (DFO) database (http://floodobservatory.colorado.edu/), a comprehensive repository of major floods documented through news reports, government records, instrumental measurements, and remote sensing sources spanning from 1985 to the present (Brakenridge, 2016). The dataset recorded times, locations, causes, and amount of affected people for each flood event. The delineation of affected

regions is illustrated through hand-drawn GIS polygons. A total of 1210 flooding events were recorded within the DFO database from 2013 to 2021 (Figure 1).

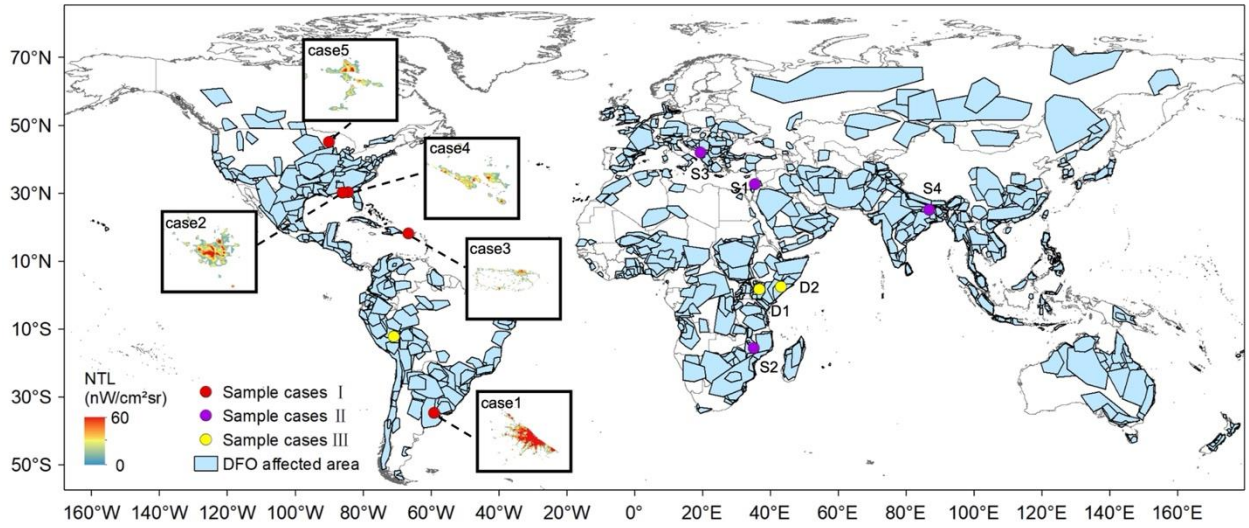

Figure 1. Hand-drawn GIS polygons of 1210 cases recorded in DFO database from 2013 to 2021; and the location for sample cases used in this research: Sample cases I for validation of NTL detectability of flood impact (Section3.3, Section4.1); Sample cases II for comparison between inundation mapping and NTL derived impact information (Section 4.2); Sample cases III for discussing reasons for NTL's non-detection of flood impact (Section5.1). The normal status light intensities of Sample cases I are shown as well.

To evaluate the uniqueness of NTL derived impact information, we conducted a comparative analysis with MODIS inundation mapping products. Ji et al (2018) generated a 500-m Resolution Daily Global Surface Water Change Database from MODIS. Compared with the other MODIS inundation datasets such as NASA MCDWD product (https://go.nasa.gov/3OiKtYB) and Global Flood Database (Tellmen et al., 2021) which only consider Red, NIR and SWIR bands and face the problem of shadows and missing data, Ji et al (2018)'s product employed an improved algorithm by 1) incorporating the Land Surface Temperature data for snow/ice exclusion, 2) utilizing all MODIS bands and setting water detection function for different types of water, 3) involving object-based post-classification to exclude shadows and 4) filling in the gaps of missing data by a temporal-spatial filtering. The product's performance was evaluated by comparison with Landsat-8 images, demonstrating that both the user's accuracy and the

producer's accuracy exceeded 93%. In this case, we employed this MODIS 500-m Resolution Daily Global Surface Water Change Database for extracting the inundation areas. This dataset is accessible through http://data.ess.tsinghua.edu.cn/modis_500_2001_2016_waterbody.html.

Country scale income groups classification from World Bank is used as development level in Section 4.4. Four groups are included in this dataset as high, middle-high, middle-low, and low income. The data can be accessed from https://data.worldbank.org. Built-up grid (GHS-Built) in 2014 from the Global human settlement layer (GHSL) data set (Pesaresi, 2023) was used for discussing the reasons for non-detection of flood impact from NTL in Section 5.1. The data provides the area ratio of built-up surface based on Landsat 8 satellite images with 30m spatial resolution.

3. Methodology

3.1.Preprocessing for Black Marble VNP46A2 NTL dataset

While substantial efforts have been dedicated to minimizing uncertainties, the VNP46A2 product still exhibits considerable unexpected daily variations due to coverage mismatch and angular effects (Román et al., 2018; Li et al., 2020; Tan et al., 2022; Wang et al., 2021). The inconsistency among daily data hinders its application, particularly for the detection of short-term events (Enenkel et al., 2020; Li et al., 2022; Román et al., 2018; Tan et al., 2022; Wang et al., 2021; Hu et al., 2024). To enhance the quality of VNP46A2 images, we employed a preprocess to exclude the two remaining errors.

Firstly, a spatial scale adjusted-average (A-average) filtering was implemented to mitigate mismatch errors, which are randomly distributed among neighboring pixels. For each pixel, we identified the annual 5% minimum light intensity after excluding outliers as the stable component (lights from the center area of the pixel), while the remaining radiance constituted the mismatch component (lights from the edge of the pixel). Subsequently, we applied a spatial average filter with a 3×3-pixel window size to the mismatch component to effectively exclude mismatch errors while minimizing blooming effects. Secondly, to address angular effects, we performed relative calibration by leveraging the periodic characteristics of the VNP46A2 product's view angle. The SNPP satellite with the VIIRS onboard is in a sun-synchronous polar orbit that repeats every 16 days. In this case, for each pixel, we separated the daily data into 16 groups according to their view angles and calculated the average light intensity. This process

yielded an angle coefficient as the ratio of the group's intensity to the annual average intensity. Dividing the daily intensity by its corresponding angle coefficient rendered light intensities coherent across varying view angles, thus excluding angular effects. The correction was systematically applied to all VNP46A2 tiles utilized in this study. Our flood impact estimation hinged upon high-quality corrected NTL images. Detailed and further information about the data correction method can be found in our published paper (Hu et al., 2024).

3.2.Estimating flood impact from NTL

Numerous indices have been devised to quantify the flood impact from the NTL data. The "Decrease Percentage" (Dp) and the "Detection Ability" (DA) are delineated by Eq.1 and Eq.2 for each pixel:

$$Dp_i = \frac{NTL_{pre} - NTL_i}{NTL_{pre}} \times 100\% \#(1)$$

$$DA_i = \frac{NTL_{pre} - NTL_i}{std_{pre}} \#(2)$$

where the NTL_{pre} and std_{pre} represent the average and standard derivation of light intensity of 100 days ahead of the flooding start date from DFO. *i* represents the date of year (hereafter doy) and NTL_i is the light intensity of the target date with doy = i. We calculated the average light intensity over the period of 100 days (about three months) as normal status (NTL_{pre}) to avoid the seasonal impact to light intensity. Light intensities within three months can be assumed as of the same season. Outlier days with intensity out of the 3×std range with the mean were excluded before calculating the indices (Pukelsheim, 1994).

The Dp index represents the magnitude of light intensity reduction compared to the normal status, indicating the serious level of flooding impact. To elucidate the severity of each case, we defined the maximum Dp observed during the flooding period as the "Severity" index. The flooding period is defined by the temporal interval spanning from the DFO-provided start time to the end time of each event. The DA index characterizes the light intensity decrease compared to the standard deviation, to facilitate comparability among different light intensity magnitudes and mitigate random noise effects. This index is instrumental in delineating the spatial extent of flood impact. We identified human settlement pixels (with light intensity > 1 nW/cm²sr) (Li et al., 2022) possessing a DA value exceeding 3 (Hu et al., 2024) as "Affected" ones, signifying that

the reduction is conspicuous enough to attribute to flooding impact rather than daily fluctuations. For the “Affected” pixels, the impact starts when DA begins to surpass 3 within the DFO-provided period of the flooding event and finishes until the DA is less than threshold 3, which indicates the light intensity is back to normal status. The temporal span of the impact for “Affected” pixels is referred to as the “Duration” index. Furthermore, we examined "unaffected" pixels when over half of their neighboring 5 x 5 pixel areas were “affected”. If these "unaffected" pixels experienced data missing due to cloud cover within the “Duration” of neighboring affected pixels, they would be categorized as "probably affected" pixels. Figure *2* shows a visual representation of these indices.

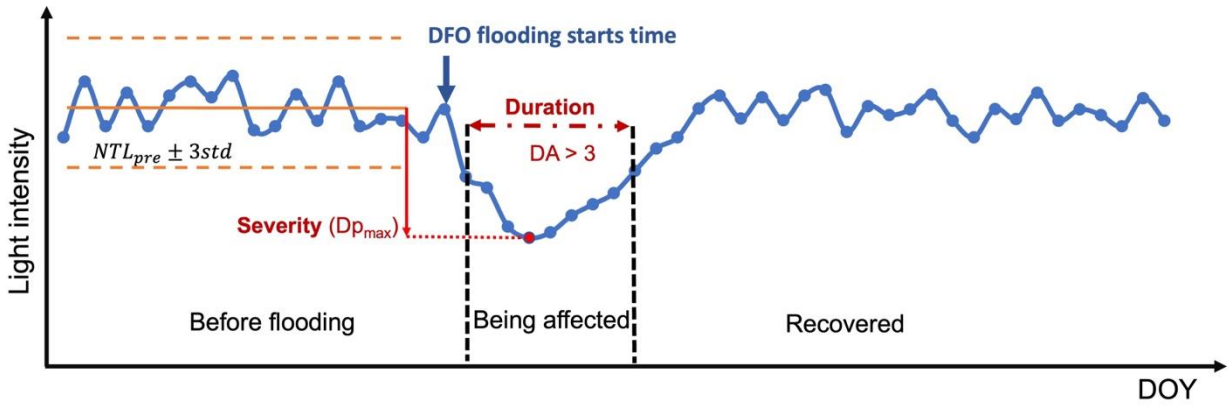

Figure 2. Schematic of light intensity variation before, during and after flooding for an affected pixel, as well as the representation of indices used to quantify flood impact through NTL images. DOY represents the day of the year.

These indices are utilized as proxies of the impact on human society and activities for flooding events. Given the potential influence of clouds on NTL images, the availability of data during the flooding period for each pixel offers a reference to gauge the reliability of impact information on a pixel scale:

$$Availability = \frac{days_{clear}}{doy_{end} - doy_{start}} \times 100\% \#(3)$$

where $days_{clear}$ represents the number of clear days during DFO-provided flooding period (doy_{start} to doy_{end}) for the target pixel. Low availability implies reduced reliability due to data

gaps stemming from cloud cover. For each event, we established the Region of Interest (hereafter ROI) as delineated by the affected polygons provided by the DFO database (Figure *1*). We calculated the flood impact indices for all human settlement pixels within the ROI.

3.3.Validation

In order to ascertain the reliability of employing NTL data for flood impact reflection, we conducted a comprehensive validation process. We selected five distinct flooding events for case studies, each of which was recorded for experiencing power outages as a direct consequence of the flooding. These specific events were chosen from the Wikipedia power outage list (https://en.wikipedia.org/wiki/List_of_major_power_outages), accessed on 20th March 2024. Impact details of the five events, including the duration and location of impact, were cross-referenced with pertinent news reports. Power outage is chosen since it leads to or is alongside with most flood impacts on human activities and society. Meanwhile, compared to other impacts, such as reductions in the industry, manufacturing, service, and public sectors, power outage events have a clearer record in the news and reports for the duration, which is useful information for validation. The location and normal status light intensity of the five cases are shown in Figure 1 (red dots). Comprehensive information is tabulated in Table 1. The Puerto Rico case (Case 3) is the most severe, extending over an exceptionally lengthy period of approximately one year. While the other events' impact lasted for 5-10 days. Three of these events were documented in the DFO database, whereas the remaining two were not. We calculated NTL flood impact indices for all five events and rigorously compared them with the recorded impact information. Moreover, we explored daily flood impact assessment with NTL data, using a single event from the DFO database as an illustrative example.

Meanwhile, prior research and applications have often relied on daytime optical remote sensing data, especially from MODIS thanks to its daily temporal resolution and long time span of historical data, to achieve near real-time inundation monitoring and exposure analysis (Tellman et al., 2021; Ji et al., 2018). To ascertain the uniqueness of NTL derived impact information, we performed a comparative analysis between the impact information derived from MODIS and NTL datasets, with a focus on 99 DFO events in 2013.

We undertook a series of preprocessing steps for Ji et al (2018)'s MODIS water surface images to facilitate their integration into our validation framework. Initially, we reprojected and

resampled (nearest neighbor resampling) the MODIS images to match the same geographic reference system (GCS) and pixel size (15 arc-second) as the NTL images, ensuring consistency across datasets. Then, we composited the MODIS images within the ROI and during the DFO provided flooding period to identify the maximum water surface area observed during the flooding event. Notably, pixels with inundation durations exceeding half a year were considered as permanent water and were subsequently excluded from our analysis. Consequently, for each flooding event, we obtained the spatial extent of the inundation and compared it with the corresponding NTL flood impact layers.

Table 1. Detailed information from news and reports for flooding cases with power outages.

	Location	Time	Description from news
Case 1 (DFO id: 4046)	Buenos, Argentina	2013.4.1	Extremely heavy rainfall caused flash floods Power shortages lasted as 15 hours for some areas, while some still have power problems until 4.6.
Case 2 (DFO id: 4393)	Tallahassee, Florida, US	2016.9.1	Hurricane Hermine swept across the Florida Panhandle, directly affecting the capital of Tallahassee. Hermine disrupted power, and 57% of homes lost power in Tallahassee, some of which were without power for a week.
Case 3 (DFO id: 4523)	Puerto Rico	2017.9.19	Hurricane with flash flooding (stemming from flood gate release at La Plata Lake Dam) destroyed the island's power grid. Some areas remained without power for 4-6 months. Power was not restored to all customers until Aug, 2018.
Case 4	Panama City, Florida, US	2018.10.10	Hurricane Michael caused flooding. Thousands of customers lost power for up to 10 days.
Case 5	Wisconsin, US	2019.7.18	Severe thunderstorms, tornadoes and floods caused damage and power outages throughout Wisconsin. Some customers were still without power a week later.

4. Results

4.1. Reliability of NTL's flood impact detection

In Figure 3, we presented the NTL impact indices for the selected flooding cases. Across all five cases, discernible reductions in light intensity are evident in the NTL images, aligning coherently with the documented information in news reports. Among the selected cases, Case 3

emerges as the most severe in terms of its impact, as corroborated by the news records. Remarkably, the NTL-derived results distinctly reflect the highest level of Severity observed for this event.

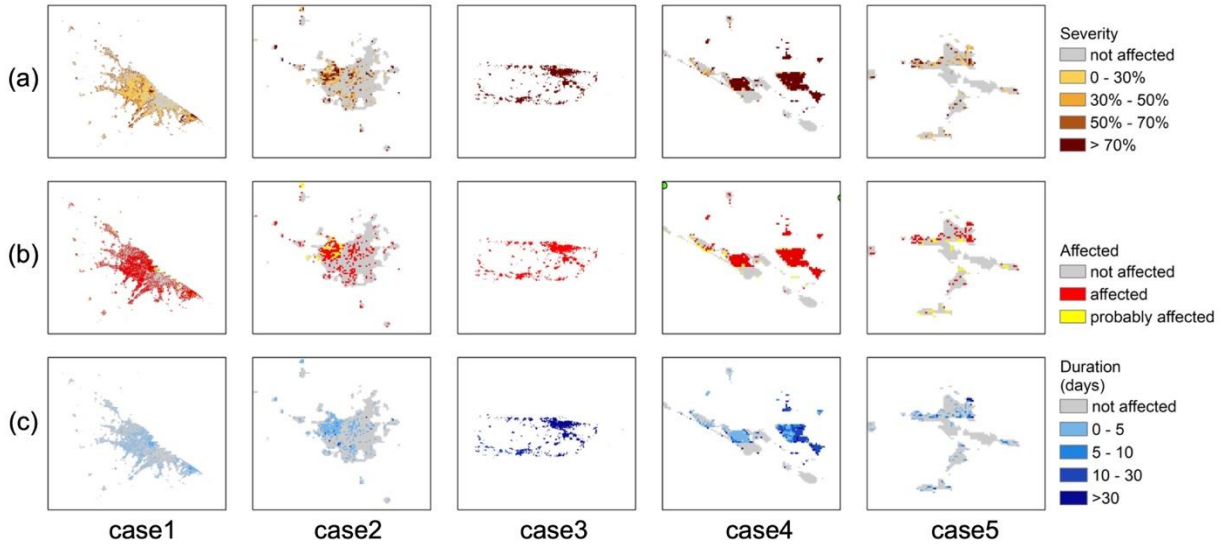

Figure 3. NTL impact indices for five selected flooding cases: (a) Severity (maximum Dp), (b) affected location and (c) duration.

In Table 2, we provided a comprehensive comparison of the durations obtained from news reports, the DFO dataset, and NTL data. To ensure comparability with reports, the highest and lowest 5% outliers were excluded from the NTL-affected Duration, representing the majority of pixels' outcomes within the flooded regions. Basically, the duration results of NTL show consistency with the reported ones for all five cases. Although the NTL duration happens to be several days shorter (Case 1) or longer (Case 4 and Case 5) compared with reports, the overall order of duration length has been well captured (Case 3 >> Case 5 > Case 4 > Case 2 > Case1). The durations documented in the DFO dataset appear to be either several days longer (Case 1 and Case 2) or considerably shorter (Case 3) than the actual power outage durations reported in news, especially evident in the severely affected Case 3. Furthermore, the DFO dataset lacks records for Case 4 and Case 5. This suggests DFO dataset might primarily record inundation rather than the impact on human society and activities. The reason might be that DFO's information heavily relies on the news and inundation mapping, focusing mainly on the

inundated period without sustained tracking of the impact on human society and activities, particularly noticeable in long term cases such as Case 3. These findings also underscore the difference between the duration of impact on human activities and the period of inundation. In Case 3, even after the inundation subsides, the residual impact on human society and activities persists for an extended period. Conversely, in Case 1 and Case 2, the impact ceases before the inundation ends, likely due to shallow inundation depths insufficient to significantly disrupt daily activities.

Table 2. Duration comparison for 5 selected cases.

	News	DFO	NTL
Case 1	15 hours to 5 days	7 days	1~3 days
Case 2	less than 1 week	8 days	1~5 days
Case 3	Weeks to 6 months	20 days	1 day ~ more than 5 months
Case 4	1 to 10 days	no record	1~ 17 days
Case 5	1 day to more than 1 week	no record	1 ~ 14 days

Figure 4 shows the normalized daily light intensity of all pixels within the cases' ROI, as well as the median intensity for each date. The original light intensity was normalized by the annual mean value of each pixel for better visualization of pixels with different intensity magnitudes. For all five cases, the light intensity can be observed as reducing after flooding occurs and gradually increasing to its normal status. Moreover, for Case 4 and Case 5, which have recorded relatively longer periods of power outage compared to Case 1 and Case 2, the durations detected by NTL are longer than the reported power outage. These results confirm that NTL can detect slowdown and recovery in human and economic activity beyond power outage.

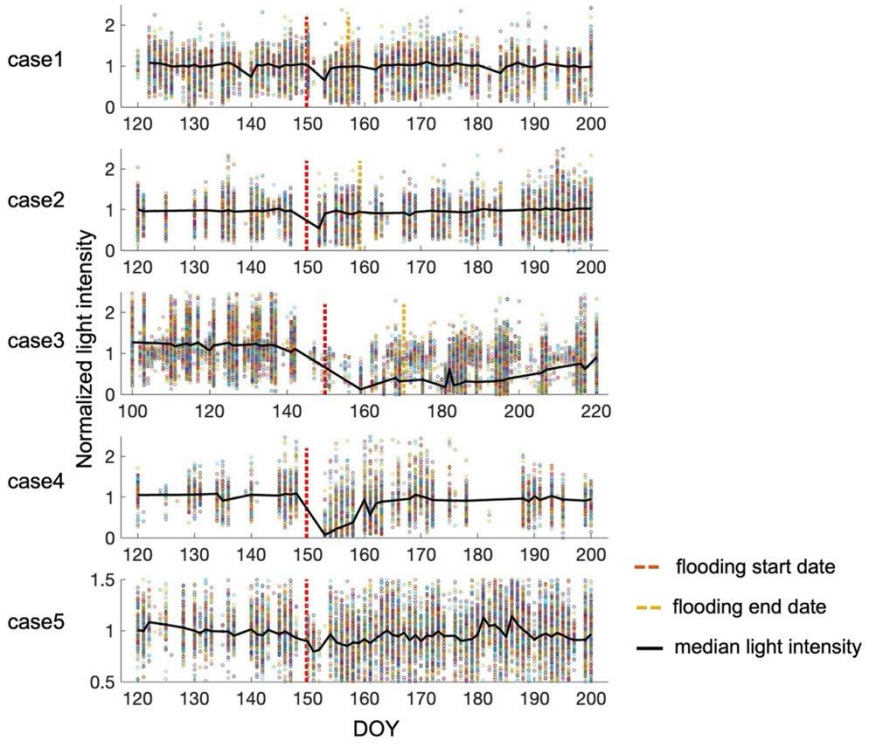

Figure 4. Normalized daily light intensity variation for pixels within five selected cases' ROI (dots), and the median value of the pixels in each day (black line). Light intensity has been normalized by the annual mean value of each pixel for better visualization of pixels with different intensity magnitudes. Dotted lines represent the flooding start and end date recorded in DFO database or news. For Case 4 and Case 5, which have not been recorded in the DFO database, only start dates are available.

The above results confirm NTL's capacity and reliability to discern flood impact. NTL could be used as a proxy for flood impact on human society and activities. Moreover, NTL data fills gaps within existing databases by addressing the impact of missing records.

4.2. Event-based daily assessment of flood impact

In Figure 5, we illustrated the daily images within the ROI for an example case recorded in the DFO database (ID: 4046, Case 1 in Section 3.3). The figure presents the daily light intensity (Figure *5* (a)) and corresponding Dp (Figure *5* (b)) during the flooding period, alongside the

baseline normal status light intensity and the Severity (maximum Dp). The normal status light intensity was derived by calculating the mean intensity over 100 days preceding the onset of flooding, with outliers — those exceeding three times the standard deviation from the mean— excluded from the calculation. The first two days of flooding were not included due to the large area of missing data caused by the cloud. The initial days (e.g., Day 3 - 5) of the event exhibit a significant decrease in light intensity, gradually recovering to the baseline magnitude over time (Day 6 -7). The daily Dp of all pixels within the event's ROI, as well as the median values, are also presented in Figure *5* (c). The median Dp is around zero before flooding. The increasing trend of Dp after flooding happened, as well as its recovery to around zero, can be well observed. These results highlight NTL's capability to reflect flood impact and effectively capture the recovery process. With 10 days' latency and daily temporal resolution of NTL product, in time daily flood impact evaluation becomes feasible, providing valuable information for post-flood impact assessment and analysis.

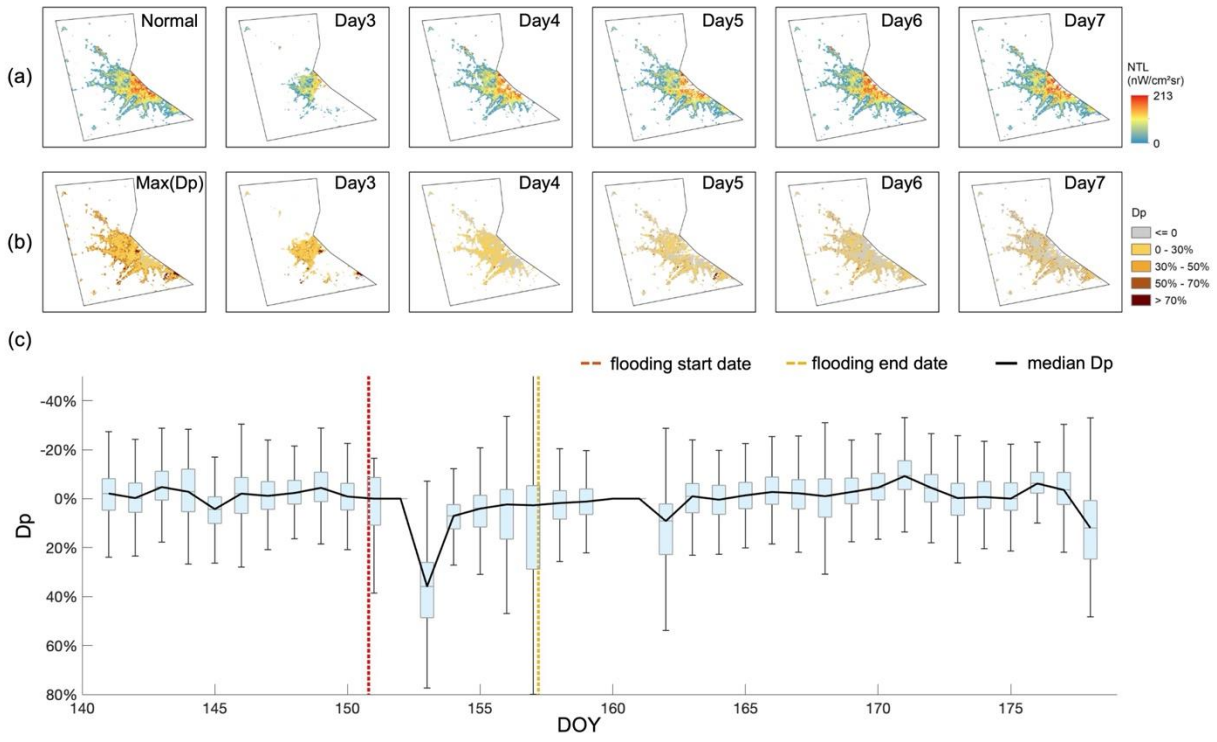

Figure 5. (a) Normal status and flooding period daily light intensity, (b) maximum and daily decrease percentage of light intensity during flooding period for an example event (DFO ID:4046), and (c) Dp variation of all pixels within the example event's ROI (box chart), and the

median Dp of the pixels in each day (black line). Dotted lines represent the flooding start and end date recorded in the DFO database.

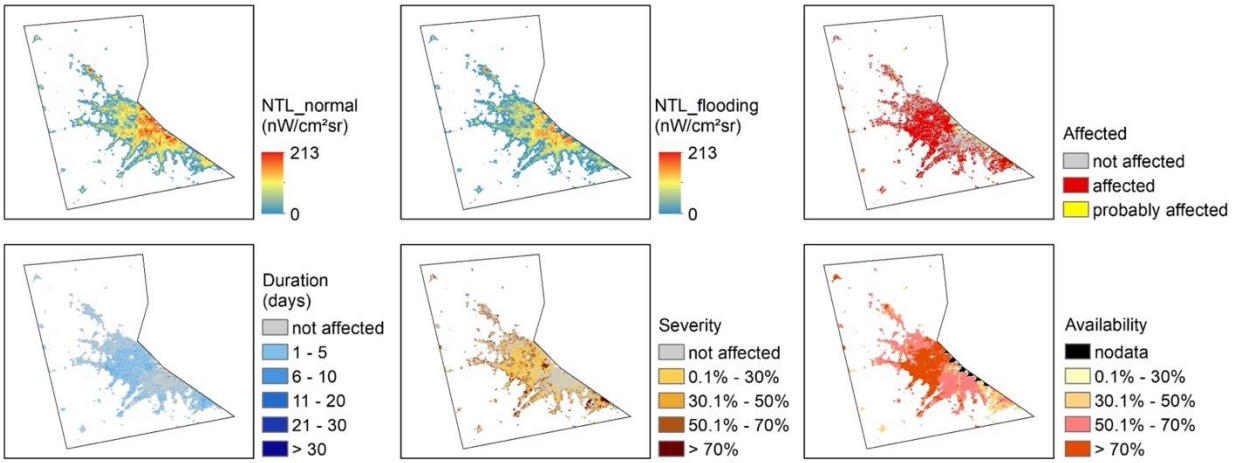

Figure 6. NTL impact layers for the example event (DFO ID: 4046) including (a) normal status light intensity, (b) minimum light intensity during flooding period, (c) affected location, (d) affected duration, (e) serious level and (f) available days' ratio during flooding period.

In Figure *6*, we present the impact layers generated from NTL images for the target event. These six layers encompass normal status light intensity, minimum light intensity during the flooding period, affected locations, impact duration, Severity, and percentage of available days during the flooding period (Availability). The Severity layers provide insight into the magnitude of impact at the pixel scale, effectively reflecting local vulnerability. The affected location could provide guidance information for protection and rescue policy making. The impact duration layer discerns the local recovery capacity. The availability layer offers a reference for assessing the pixel scale reliability of the impact layers. Across all these impact layers, spatial variability is evident for the example case. Urban areas with higher light intensities typically display fewer affected pixels, and less severe intensity decreases. Conversely, sub-urban regions emerge as the primary affected areas for this event. Observing this pattern is more straightforward when using the Severity and affected location layers generated with the proposed indices, compared to relying solely on the original light intensity. In summation, NTL data and the generated indices

efficiently deliver flood impact information on a pixel scale for each event with daily temporal resolution. This pixel-scale information is important for delineating local variability in vulnerability and recovery capacity. The simplicity of the NTL flood impact indices allows for the efficient generation of such impact layers for historical events and immediately after flooding happens. This capability facilitates long-term large-scale flood impact analysis and timely evaluation of the latest flooding events.

4.3.Comparison between NTL impact information and inundation mapping

We examined 99 events in 2013, of which 94 were detected as having inundation from MODIS data. For 75 of these events, available pixels within the DFO ROI during the flooding period were identified, and 70 exhibited a decrease in light intensity detected from NTL. In 21 cases, inundation and NTL detected affected areas overlapped with each other.

For some cases, little inundation area was detected in MODIS data despite DFO records indicating people were affected. In Figure *7*, Case S1 and S2 have 0% and 0.2% inundated within the ROI, while DFO records 1602 and 3003 people affected. This highlights instances where MODIS failed to detect inundation, suggesting that there was no corresponding affected area from inundation mapping. Conversely, NTL successfully captured 38.5% and 89.1% affected areas within human settlement regions for Case S1 and S2, which shows consistency with DFO records. Furthermore, even for cases in which both inundation mapping and NTL data detected affected areas, differences in impact between the two datasets were observed. In Figure 7, Case S3 and S4, substantial disparities in the affected locations between the two datasets were evident. MODIS inundation areas typically aligned with river proximity, while NTL affected areas were concentrated within human settlements.

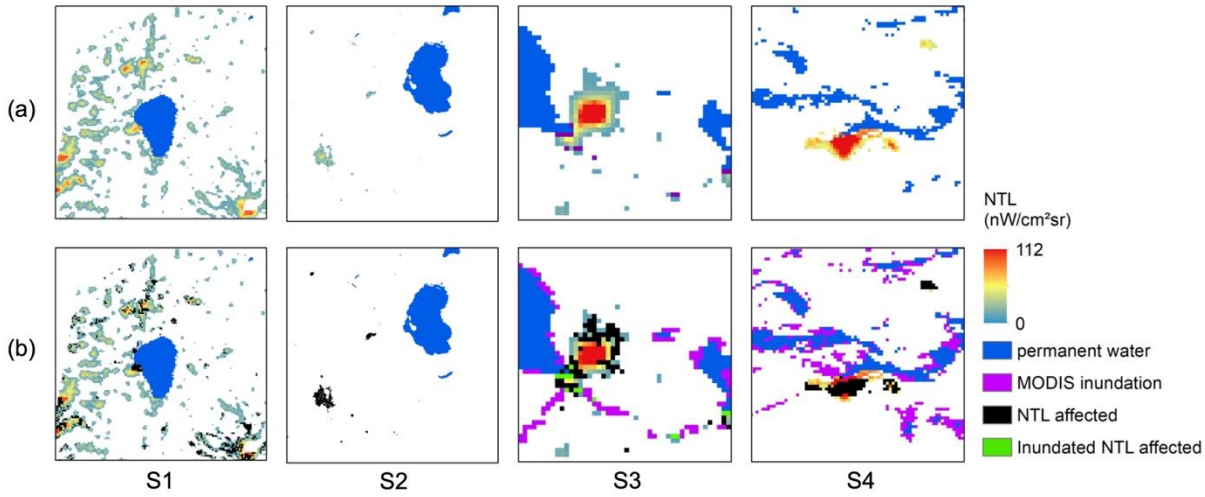

Figure 7. Comparison of MODIS inundation and NTL detected affected area for 4 sample events recorded in DFO. (DFO ID and located country for case S1: 4019, Palestine; case S2: 4021, Malawi; Case S3: 4047, Albania; Case S4: 4098, India). (a) Light intensity and permanent water within DFO ROI; (b) flooding affected area detected by MODIS inundation, NTL data and both.

In Figure 8, we present the statistical results depicting the overlapping ratio of NTL affected areas and MODIS inundation for the 99 events in 2013. Remarkably, less than 3.5% of the NTL affected area coincided with observed inundation (Figure 8 (a)), further validating that a significant portion of impact occurs outside of inundation areas. Meanwhile, the ratio of NTL detected affected human settlement areas within inundated one ranges from 1% to 60% (Figure 8 (b)), suggesting that not all inundated areas necessarily experience a significant impact on human society. For some areas, shallow inundation depth may be insufficient to cause noticeable disruption in human daily life.

These results indicate NTL's capacity to fill in the gap left by inundation mapping and provide new insights into flood impacts beyond inundation areas, affecting human society and activities. NTL-derived impact can enhance understanding of the diverse impacts both within and outside inundation areas. There exist five events that has not been detected as having impact by NTL in 2013. The reasons for non-detection have been further explored in Section 5.1.

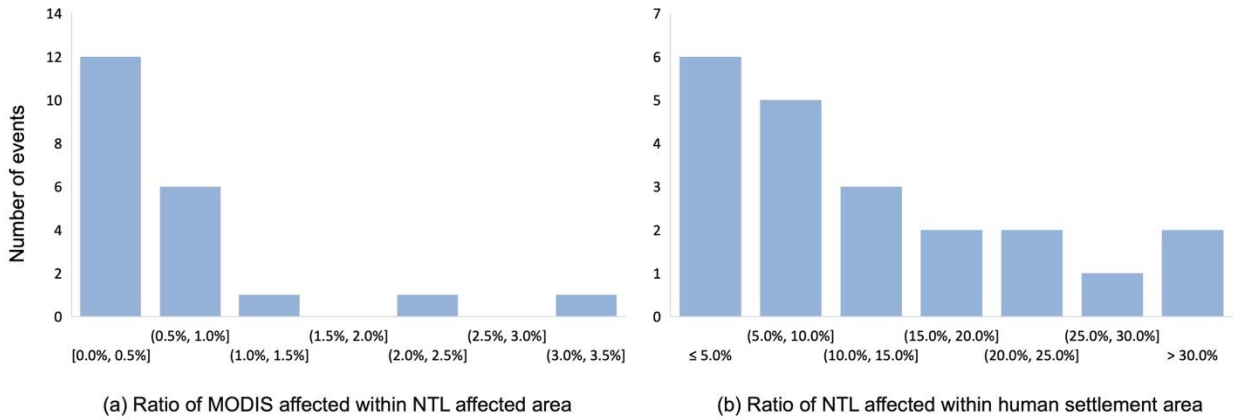

Figure 8. Statistical analysis result for the overlapping of NTL detected affected area and MODIS inundation area. Events amount distribution for (a) the ratio of inundated area within the NTL detected affected area and (b) the ratio of inundated affected area within the inundated human settlement area.

We conducted a further comparison between the Dp of flood impacts detected by NTL within and out of the inundated area (Figure 9). 13 events (ID 4019, 4023, 4046, 4047, 4050, 4063, 4064, 4071, 4089, 4091, 4092, 4101, 4109) exhibited higher Dp within inundated areas. The rest eight events showed slightly higher Dp outside of inundation. However, the difference is not large between Dp within and outside inundation areas for all 21 events. This suggests that impacts are of comparable magnitude and importance within and outside of the inundation area. NTL data, therefore, plays a crucial role in supplementing flood impact information beyond inundation, which is equally vital alongside impacts within inundated regions.

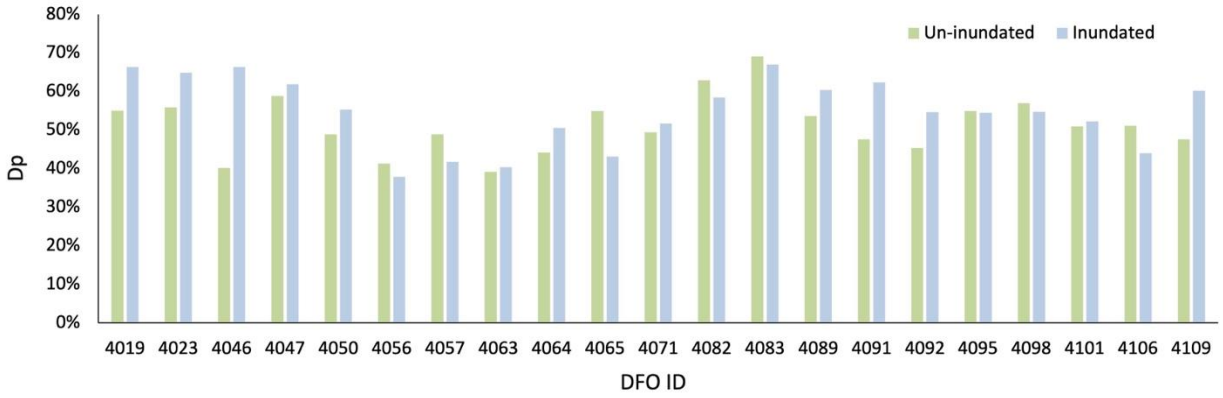

Figure 9. Comparison of Dp of pixels within and beyond inundation for 21 events in 2013, which has an overlap between the NTL-detected affected area and the MODIS inundation area.

4.4.Flood impact analysis on the global scale for the recent decade (2013 – 2021)

With NTL imagery, we generated NTL flood impact layers for historical global flooding events occurring in the recent decade (2013-2021) as recorded in the DFO database. Out of the total 1,120 recorded cases, 90 have no human settlement area within the DFO ROI, while 154 were hindered by cloud cover, rendering them unsuitable for analysis. From the remaining 876 events, 72 exhibited no discernible flood impact from NTL. NTL impact indices images for 804 events have been generated with a spatial resolution of 15 arc-second.

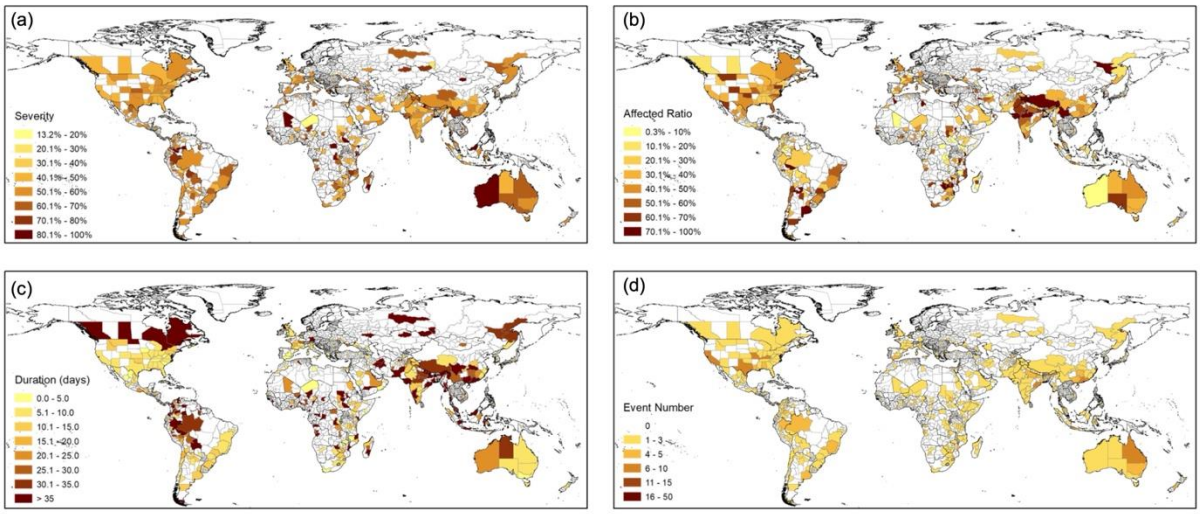

Figure 10. Global map showing the flood impact from NTL in terms of (a) Severity, (b) the ratio of affected area within human settlement (Affected Area Ratio), and (c) affected Duration for 876 events recorded in the DFO database from 2013 to 2021. Event numbers are shown in (d) for each administrative unit.

Figure 10 offers a spatial visualization of the flood impact derived from NTL data, including Severity, Affected Area Ratio, Duration, and flood occurrence time on the administrative level. In general, the Duration, which signifies the recovery process, appears to correlate with both the Severity and Affected Area Ratio. For example, in northeast Brazil, Paraguay, Canada, and China, there is a relatively higher Severity or Affected Area Ratio; the Duration for these areas is correspondingly longer as well compared to the other areas. While for North Africa (e.g., Sudan, Niger) and some parts of Europe (e.g., Spain, France), the Severity and Affected Area Ratio, as well as the Duration, are all lower. Such a tendency is reasonable since a more substantial reduction in light intensity and a broader affected area tend to result in a longer time for recovery. However, intriguing outliers exist. Regions such as the United States and East South America (including Argentina and southwest Brazil) exhibit lower Duration, indicating faster recovery rates, despite possessing similar Severity and affected area values compared to other areas. For Australia, the east part has a higher Affected Area Ratio but lower Severity and Duration compared to the west part. This phenomenon can be attributed to concentrated urban

development in the east part. The higher population density, hence, leads to a larger affected area ratio. However, greater economic development ensures a better defense ability and quicker recovery. Conversely, regions like Khanty and Khabarovsk in Russia and Middle Africa have similar Severity and affected area ratio magnitudes but exhibit higher Duration values compared to other regions, implying a slower recovery rate. The spatial pattern seems closely tied to local economic development, with the United States, Brazil, and East Australia boasting high incomes while Khanty, Khabarovsk, and Middle Africa register relatively lower income levels.

Aside from the influence of local development, the severity of flooding may also influence the magnitude of flood impact. Thus, we conducted a comprehensive statistical analysis of impact across different development and flood severity levels, as illustrated in Figure 11. The DFO's provided serious index was incorporated to gauge flood severity. Event numbers for different development and flood severity groups are shown in Table S1. Our findings indicate a general trend for impact Severity and Duration: as development levels rise, these factors tend to decrease. This suggests that highly developed regions have lower vulnerability and better recovery capabilities compared to less developed areas. The decrease in group upper values is significant as development levels increase, especially for the Duration in the low development group when DFO_serious equals 3. This implies that extremely severe and long-lasting impacts are more likely to occur in regions with lower levels of development, while they can be avoided in higher development areas. Some exceptions were observed within the low development group when DFO_serious equals 1 and 1.5. In these cases, the Duration and Affected Area Ratio were even lower compared to that in the middle-low group. This discrepancy may be attributed to the NTL's reduced ability to detect impact in areas with low illumination (see more in Section 5.1).

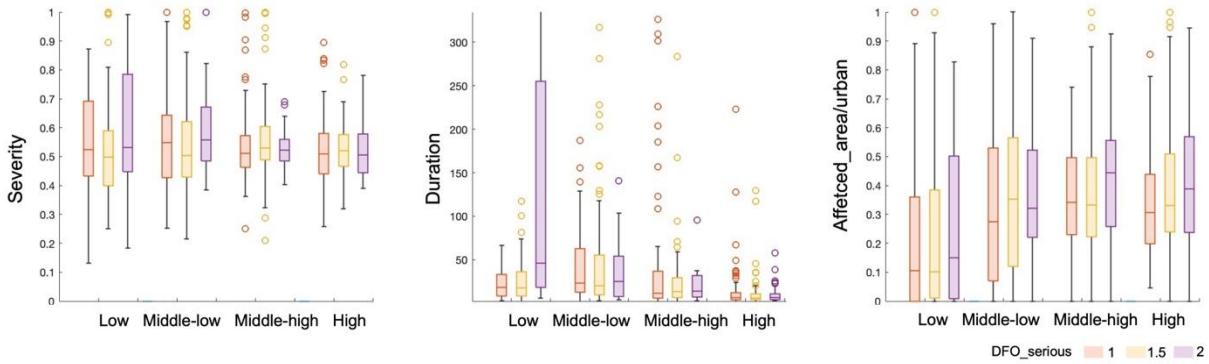

Figure 11. Comparison of NTL flood impact indices (Severity, Duration, and Affected Area Ratio) for events with different serious levels from DFO located in countries with different GDP levels.

Impact levels for events located in high-income regions tend to be concentrated with similar magnitudes. In contrast, for low-income regions, the impact magnitude for different events varies significantly, indicating substantial differences in local defense and recovery capabilities. The reason might be that in some regions, despite lower development levels, frequent disasters improve the local resilience and adaptability to flooding. Additionally, the magnitudes of impact among different flooding severity levels vary more with development decreases. For well-developed regions, the impact always remains at a low level with different flooding severities. While for the low developed regions, when the flooding becomes more serious, the impact increases as well, especially for Duration. This indicates that in low-income areas, recovery after severe flooding is notably challenging.

5. Discussion

5.1.Reasons for non-detection of flood impact from NTL

Out of the 876 global-scale events from 2013 to 2021 analyzed in this study, 72 were not detected as having a flood impact using NTL data. We investigated the characteristics of these undetected events and found some compelling reasons for their non-detection.

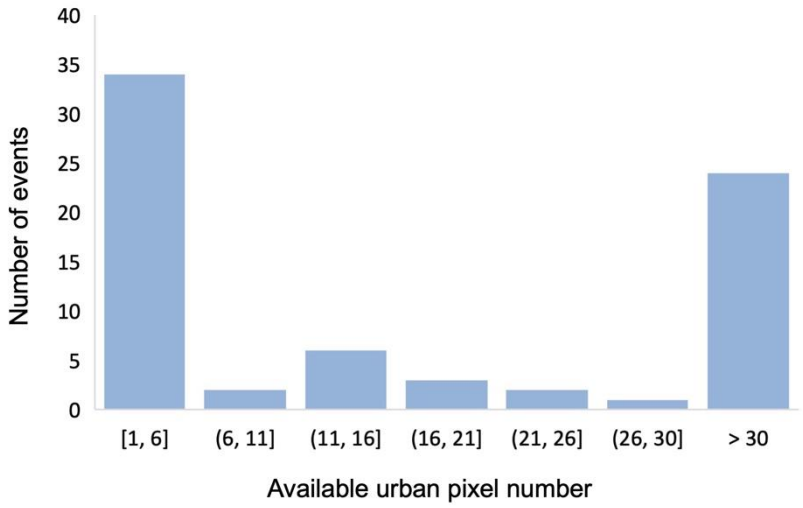

Figure 12. Number of events for different amount of available urban pixels within the DFO given polygon during flooding period.

Firstly, 67% (48 events) of the undetected cases had fewer than 30 available urban pixels within the DFO defined ROI (Figure 12). The limited number of urban pixels likely contributed to the misdetection of flood impacts. Furthermore, upon closer examination of the remaining 24 undetected events, we observed that they were primarily located in low-light areas in underdeveloped countries or suburban regions. Figure 13 illustrates the human settlement area ratio from the GHSL dataset, light intensity, and DA layers for three events that were not detected as having impacts but had a sufficient number of available human settlement pixels. In these cases, human settlement exhibits a dispersed pattern within less well-developed urban areas (Figure 13 (a) (b)). Although there was an obvious decrease in light intensity during the flood period (Figure *13* (c) (d)), no pixels were detected as impacted. This suggests that the DAs for all pixels during the flooding period are smaller than 3 (Figure *13* (e)), possibly due to a large standard deviation (std) caused by unstable power supply systems in underdeveloped countries, such as Somalia. Another reason for non-detection could be that the pixels were not part of the human settlement, but rather other sources of light, such as wildfires, which are not stable and thus have higher std. Moreover, cloud-induced data gaps also contributed to the unavailability of large areas of human settlement data, which affected detection. This was also compounded by the low accuracy of the DFO-provided ROI, which did not always encompass the main potentially affected human settlement regions but focused more on inundation-related areas

(Figure 13 (a)). Another reason might be that flooding did not significantly impact human society and activities. In cases like these, such as events 4304, 4391, 4582, and 4895, the number of affected individuals recorded in the DFO database was minimal, suggesting that the actual impact was weak (Table S2).

Figure 13. (a) Built-up area ratio, (b) normal status light intensity within ROI, (c) normal status light intensity, (d) minimum light intensity during flooding period, and (e) DA layers within the enlarged area within the red rectangle for three example cases (DFO ID and located country for case D1: 4955, Kenya; case D2: 4981, Somalia; case D3: 5043, Peru) that have not been detected having an impact from NTL.

5.2.Relationship among the NTL impact information, inundation mapping and DFO database

Investigative databases like DFO serve as primary sources for obtaining information on the impact of historical global flooding events. Inundation data also plays a crucial role in flood risk estimation globally and serves as a reference for assessing near real-time flood impacts. This study employed NTL data to estimate the impact of flooding on human society and activities. We'd like to explore the relationships among NTL derived impact information, inundation mapping as well as the DFO database. We analyzed 99 cases from 2013 to examine the impact from the three datasets and classify the cases accordingly. We generated confusion matrices and

584 calculated the overall accuracy of classification to assess the consistency between the different
585 datasets regarding flood impact (Figure 14, Figure 15).
586 Our findings revealed a strong consistency (80% as overall accuracy) between the DFO-
587 recorded duration and MODIS-observed duration, indicating that the DFO database primarily
588 records inundation duration rather than the impact duration on human activities. For the DFO-
589 recorded severity level and affected population, the NTL-observed affected area and severity
590 level have the highest correlation separately (48%). The results suggest that, in comparison to
591 inundation data, NTL data is more closely related to the human-related impact, such as the
592 affected population. Furthermore, NTL's severity level also exhibited a relatively high
593 consistency with inundation duration (50.67% as overall accuracy), implying that the duration of
594 inundation directly affects the impact on human society and activities. However, DFO-recorded
595 severity level and NTL-observed affected area, DFO affected population and NTL severity level
596 are still not strongly correlated with the overall accuracy of 48%. The reason may be that for
597 some cases, the DFO records' numbers are rough estimations from news, which largely reduces
598 the accuracy.
599 In summary, these three datasets capture flood impact from various perspectives. DFO
600 primarily records information such as location, timing, estimated affected populations, and
601 severity based on news descriptions. Its advantage lies in its long-time period records spanning
602 from 1985 to the present, along with its provision of tentative affected regions for each event.
603 However, the impact information from DFO, including affected populations and severity, relies
604 on descriptions from news sources and is, therefore, subject to lower accuracy. MODIS
605 inundation data provides information on the daily area and duration of inundation, contributing
606 to monitoring water variations during flooding events. NTL provides daily information on the
607 affected location, severity and duration of each event within and beyond the inundation areas.
608 The NTL impact layers focus on human settlement areas, which can be as proxies for impacts on
609 human society and activities. With the NTL derived flood impact information, it is possible to
610 further estimate flooding cost (e.g., economic loss or affected fatalities). Combining these
611 datasets offers a more comprehensive understanding of flood impacts worldwide.
612

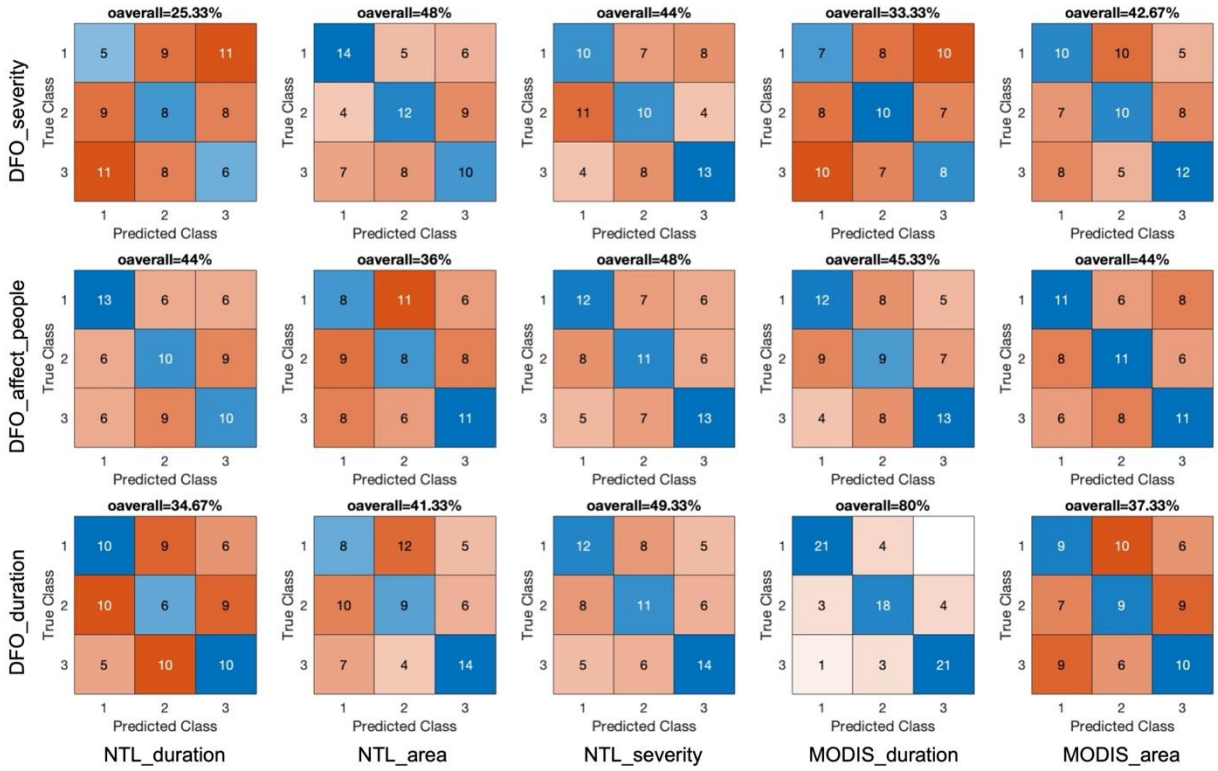

Figure 14. Confusion matrix and overall accuracy of DFO and NTL, MODIS classification.

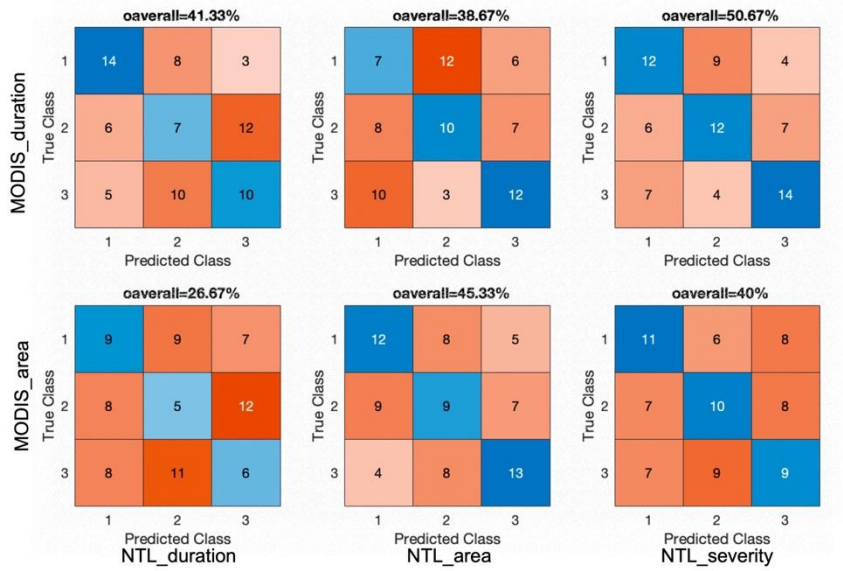

Figure 15. Confusion matrix and overall accuracy of MODIS and NTL classification

5.3.Advantages and limitations

In this study, we harnessed NTL data to estimate the impact of flooding on human society and activities. The global impact was analyzed for 876 historical events occurring from 2013 to 2021. The impact information derived from NTL serves as a valuable tool for discussing how flooding leads to residential buildings' damage, displacement and fatalities, interruptions on the industry, service, and public sectors, which cause variations in light intensity. When floods destroy buildings and devastate power supply chains, many human settlements are left without power, significantly affecting normal daily activities. Additionally, fatalities and displacement due to flooding result in previously inhabited areas lacking inhabitants. Floods can also hinder factory operations, leading to reduced production efforts. Commercial zones, such as markets, as well as public regions, such as schools and hospitals, might be closed due to flooding caused by power outages or shortages of essential materials. Such impacts reduce the light intensity of corresponding regions and can be effectively observed through NTL data, even on a large scale. All these impacts are closely tied to human society and are of interest to policymakers, operators, and insurers to evaluate and mitigate asset and life losses, maintain socioeconomic stability, and to reduce risk exposure and liabilities (Koks et al., 2019). The information on these impacts has not been fully explored using existing methods or datasets on a global scale, especially for those out of the inundation area. Our estimations bridged this gap and provided a complete understanding of flood impact both within and beyond inundation areas on human society.

Meanwhile, compared to previous studies focusing on potential impact, which assumes all people and assets within the inundation area are affected with various serious levels considering inundation depth (Winsemius et al., 2013), NTL reflects flood impact from actual light intensity variation. This approach can provide more realistic affected location and severity information, especially on a global scale. Furthermore, in contrast to studies that assume recovery duration has a linear relationship with inundation duration (Tanoue et al., 2020; Taguchi et al., 2022), NTL reveals a recovery process from light intensity, which is more rational. Meanwhile, the simplicity of the NTL flood impact indices allows for the efficient generation of impact layers for historical events and immediately after flooding happens. Large-scale flood impact analysis can be achieved with less complexity. In time, daily impact assessment can be achieved with the high-quality uncertainties corrected VNP46A2 NTL product, which facilitates post-flooding impact analysis and tracking of daily variations in impacts. Pixel-scale vulnerability and

resilience, loss estimation after flooding, as well as the locations and destinations of displacement, can be further investigated to furnish valuable insights into the flood impact on human society on a global scale. Additionally, despite the VNP46 suite used in this study, a near real-time product (Black Marble NRT) without uncertainties correction is also provided, which has a shorter (three to five hours) latency compared to VNP46A2 (10 days). Near real-time impact assessment is possible with the NRT NTL product with three to five hours' latency (Roman et al., 2018; Zheng et al., 2023). Even though the NRT NTL product carries uncertainties due to moonlight, BRDF, seasonal change etc., it holds the potential to provide rough but crucial information for emergency guidance.

There are some limitations in this study. NTL, as a proxy of flood impact, might miss or overestimate flood impact. The impact that does not cause light intensity variation cannot be well detected, e.g., damage to facilities with no light at night. However, since NTL has been proven to well reflect human activities (Elvidge et al., 2001; Li et al., 2022; Zheng et al., 2022), it still can cover a large portion of the impact, especially the one related to human society and activities. Other events that reduce the light intensity other than flooding might exist, which leads to overestimation from NTL. Since we have employed the DFO-provided flooding period for impact detection with NTL, the possibility of overestimation can be largely reduced. We established a threshold of 3 for the DA index to identify affected pixels. The extent of the affected area can vary with different thresholds. However, since we also provide the DA layer, users have the flexibility to adjust the threshold to align with their research objectives. A major challenge in flood impact estimation using NTL data is the presence of cloud cover, particularly during flooding events caused by heavy rain or storms. As demonstrated by our results, from 2013 to 2021, cloud cover rendered 26% of the recorded events (292 out of a total of 1120 events) undetectable through NTL due to cloud obstructions. For such events, estimating impact through NTL may be difficult, but the subsequent recovery situation can still be assessed. We anticipate the development of models that can address gaps caused by cloud cover or combine data from different satellites to mitigate this cloud-related issue. Moreover, the performance of using NTL to detect flood impact may be suboptimal in low-light areas, posing a particular challenge for underdeveloped countries. However, for most countries, NTL performance is likely to improve over time as development progresses.

6. Conclusion

This study proposed an innovative approach to flood impact evaluation with high-quality NTL remote sensing data. Results have confirmed the reliability of NTL flood impact through case studies. The affected durations derived from NTL show higher consistency with the reported flood impact duration for the five selected cases compared with the DFO database, which is more related to inundation duration. The recovery process can be well captured from NTL data. The generated impact indices provide the affected Severity, location and Duration on pixel scale both within and beyond the inundation areas. Daily assessment of flood impact for flooding events can be realized efficiently with these indices on a large scale.

Compared to traditional inundation mapping, NTL data offers a unique perspective, focusing on human settlements. Only 21 of the 99 events in 2013 show overlap of NTL detected affected area with satellite-based inundation, with a ratio less than 3.5% to the NTL affected area coincided with MODIS observed inundation. Meanwhile, NTL-observed affected area and Severity level have a higher correlation with DFO recorded severity level and affected population compared to MODIS inundation area and duration. These results indicate that a significant portion of impact occurs outside of satellite-based inundation areas, emphasizing the significance of NTL's detection for impact both within and beyond inundation areas on human society and activities.

Over the study period from 2013 to 2021, we generated NTL impact layers for 876 events sourced from the DFO with a spatial resolution of 15 arc-second (about 500 m). Based on the detected events, we analyzed the global spatial patterns of flood impact in terms of Severity, Duration, and Affected Area Ratio. The magnitude of these indices varies significantly by location, reflecting diverse levels of vulnerability and recovery capabilities. The spatial distribution is influenced by local economic development and flood severity.

In summary, our study has demonstrated that NTL data can effectively assess flood impact on human society within and beyond inundation areas. It provides a foundation for impact monitoring and the exploration of local vulnerability and resilience in the face of flooding. NTL flood impact information can be an important supplement to give a more comprehensive understanding of flood impact on a global scale. This information is expected to serve as a critical tool for emergency response, policy formulation, and decision-making for government and insurance companies.

CRediT authorship contribution statement

Yang Hu: Conceptualization, Methodology, Software, Validation, Formal analysis, Visualization, Writing. Dai Yamazaki: Conceptualization, Methodology, Validation, Formal analysis, Writing, Funding acquisition. Xudong Zhou: Conceptualization, Methodology, Formal analysis, Writing. Gang Zhao: Conceptualization, Methodology, Formal analysis, Writing.

Declaration of Competing Interest

The authors declare that they have no known competing financial interests or personal relationships that could have appeared to influence the work reported in this paper.

Acknowledgments

This research was partially supported by NEDO [JP21500379] and Ministry of the Environment of Japan [JPMEERF23S21130]. Yang Hu is supported by Scholarship from China Scholarship Council.

Reference

Ciscar, J.-C., Iglesias, A., Feyen, L., Szabó, L., Van Regemorter, D., Amelung, B., et al. (2011). Physical and economic consequences of climate change in Europe. *Proceedings of the National Academy of Sciences*, *108*(7), 2678–2683. https://doi.org/10.1073/pnas.1011612108

Dottori, F., Szewczyk, W., Ciscar, J.-C., Zhao, F., Alfieri, L., Hirabayashi, Y., et al. (2018). Increased human and economic losses from river flooding with anthropogenic warming. *Nature Climate Change*, *8*(9), 781–786. https://doi.org/10.1038/s41558-018-0257-z

Elvidge, C. D., Baugh, K. E., Kihn, E. A., Kroehl, H. W., Davis, E. R., & Davis, C. W. (1997). Relation between satellite observed visible-near infrared emissions, population, economic activity and electric power consumption. *International Journal of Remote Sensing*, *18*(6), 1373–1379. https://doi.org/10.1080/014311697218485

Elvidge, Christopher D, Imhoff, M. L., Baugh, K. E., Hobson, V. R., Nelson, I., Safran, J., et al. (2001). Night-time lights of the world: 1994–1995. *ISPRS Journal of Photogrammetry and Remote Sensing*, *56*(2), 81–99. https://doi.org/10.1016/S0924-2716(01)00040-5

Enenkel, M., Shrestha, R. M., Stokes, E., Roman, M., Wang, Z., Espinosa, M. T. M., et al. (2020). Emergencies do not stop at night: Advanced analysis of displacement based on satellite-derived nighttime light observations. *IBM Journal of Research and Development*, *64*(1/2), 8:1-8:12. https://doi.org/10.1147/JRD.2019.2954404

G.R. Brakenridge. (2016). Global Active Archive of Large Flood Events. Dartmouth Flood Observatory, University of Colorado, USA. http://floodobservatory.colorado.edu/ Archives/

Hu, Y., Zhou, X., Yamazaki, D., & Chen, J. (2024). A self-adjusting method to generate daily consistent nighttime light data for the detection of short-term rapid human activities. *Remote Sensing of Environment*, *304*, 114077. https://doi.org/10.1016/j.rse.2024.114077

IPCC Managing the Risks of Extreme Events and Disasters to Advance Climate Change Adaptation (Cambridge Univ. Press, 2012); http://ipcc-wg2.gov/SREX/report

Ji, L., Gong, P., Wang, J., Shi, J., & Zhu, Z. (2018). Construction of the 500-m Resolution Daily Global Surface Water Change Database (2001–2016). *Water Resources Research*, *54*(12). https://doi.org/10.1029/2018WR023060

Jongman, B., Kreibich, H., Apel, H., Barredo, J. I., Bates, P. D., Feyen, L., et al. (2012). Comparative flood damage model assessment: towards a European approach. *Natural Hazards and Earth System Sciences*, *12*(12), 3733–3752. https://doi.org/10.5194/nhess-12-3733-2012

Jongman, Brenden, Ward, P. J., & Aerts, J. C. J. H. (2012). Global exposure to river and coastal flooding: Long term trends and changes. *Global Environmental Change*, *22*(4), 823–835. https://doi.org/10.1016/j.gloenvcha.2012.07.004

Jongman, Brenden, Winsemius, H. C., Aerts, J. C. J. H., Coughlan De Perez, E., Van Aalst, M. K., Kron, W., & Ward, P. J. (2015). Declining vulnerability to river floods and the global benefits of adaptation. *Proceedings of the National Academy of Sciences*, *112*(18). https://doi.org/10.1073/pnas.1414439112

Jonkman, S. N., Bočkarjova, M., Kok, M., & Bernardini, P. (2008). Integrated hydrodynamic and economic modelling of flood damage in the Netherlands. *Ecological Economics*, *66*(1), 77–90. https://doi.org/10.1016/j.ecolecon.2007.12.022

Koks, E., Pant, R., Thacker, S., & Hall, J. W. (2019). Understanding Business Disruption and Economic Losses Due to Electricity Failures and Flooding. *International Journal of Disaster Risk Science*, *10*(4), 421–438. https://doi.org/10.1007/s13753-019-00236-y

Li, T., Zhu, Z., Wang, Z., Román, M. O., Kalb, V. L., & Zhao, Y. (2022). Continuous monitoring of nighttime light changes based on daily NASA's Black Marble product suite. *Remote Sensing of Environment*, *282*, 113269. https://doi.org/10.1016/j.rse.2022.113269

Merz, B., Kreibich, H., Schwarze, R., & Thieken, A. (2010). Review article "Assessment of economic flood damage" *Natural Hazards and Earth System Sciences*, *10*(8), 1697–1724. https://doi.org/10.5194/nhess-10-1697-2010

Pesaresi, M. (2023). GHS-BUILT-S R2023A - GHS built-up surface grid, derived from Sentinel2 composite and Landsat, multitemporal (1975-2030) [Data set]. [object Object]. https://doi.org/10.2905/9F06F36F-4B11-47EC-ABB0-4F8B7B1D72EA

Pukelsheim, F. (1994). The three sigma rule. *The American Statistician*, *48*(2), 88–91.

Román, M. O. (n.d.). Black Marble User Guide (Version 1.2).

Román, M. O., Wang, Z., Sun, Q., Kalb, V., Miller, S. D., Molthan, A., et al. (2018). NASA's Black Marble nighttime lights product suite. *Remote Sensing of Environment*, *210*, 113–143. https://doi.org/10.1016/j.rse.2018.03.017

Smith, K., & Ward, R. (1998). *Floods: physical processes and human impacts.*

Taguchi, R., Tanoue, M., Yamazaki, D., & Hirabayashi, Y. (2022). Global-Scale Assessment of Economic Losses Caused by Flood-Related Business Interruption. *Water*, *14*(6), 967. https://doi.org/10.3390/w14060967

Tan, X., Zhu, X., Chen, J., & Chen, R. (2022). Modeling the direction and magnitude of angular effects in nighttime light remote sensing. *Remote Sensing of Environment*, *269*, 112834. https://doi.org/10.1016/j.rse.2021.112834

Tanoue, M., Taguchi, R., Nakata, S., Watanabe, S., Fujimori, S., & Hirabayashi, Y. (2020). Estimation of Direct and Indirect Economic Losses Caused by a Flood With Long-Lasting Inundation: Application to the 2011 Thailand Flood. *Water Resources Research*, *56*(5), e2019WR026092. https://doi.org/10.1029/2019WR026092

Tellman, B., Sullivan, J. A., Kuhn, C., Kettner, A. J., Doyle, C. S., Brakenridge, G. R., et al. (2021). Satellite imaging reveals increased proportion of population exposed to floods. *Nature*, *596*(7870), 80–86. https://doi.org/10.1038/s41586-021-03695-w

Wang, Z., Román, M. O., Sun, Q., Molthan, A. L., Schultz, L. A., & Kalb, V. L. (2018). MONITORING DISASTER-RELATED POWER OUTAGES USING NASA BLACK MARBLE NIGHTTIME LIGHT PRODUCT. *The International Archives of the Photogrammetry, Remote Sensing and Spatial Information Sciences*, *XLII–3*, 1853–1856. https://doi.org/10.5194/isprs-archives-XLII-3-1853-2018

Wang, Zhuosen, Román, M. O., Kalb, V. L., Miller, S. D., Zhang, J., & Shrestha, R. M. (2021). Quantifying uncertainties in nighttime light retrievals from Suomi-NPP and NOAA-20 VIIRS Day/Night Band data. *Remote Sensing of Environment*, *263*, 112557. https://doi.org/10.1016/j.rse.2021.112557

Winsemius, H. C., Van Beek, L. P. H., Jongman, B., Ward, P. J., & Bouwman, A. (2013). A framework for global river flood risk assessments. *Hydrology and Earth System Sciences*, *17*(5), 1871–1892. https://doi.org/10.5194/hess-17-1871-2013

Zhao, X., Yu, B., Liu, Y., Yao, S., Lian, T., Chen, L., et al. (2018). NPP-VIIRS DNB Daily Data in Natural Disaster Assessment: Evidence from Selected Case Studies. *Remote Sensing*, *10*(10), 1526. https://doi.org/10.3390/rs10101526

Zheng, Q., Weng, Q., Zhou, Y., & Dong, B. (2022). Impact of temporal compositing on nighttime light data and its applications. *Remote Sensing of Environment*, *274*, 113016. https://doi.org/10.1016/j.rse.2022.113016

Zheng, Q., Seto, K. C., Zhou, Y., You, S., & Weng, Q. (2023). Nighttime light remote sensing for urban applications: Progress, challenges, and prospects. *ISPRS Journal of Photogrammetry and Remote Sensing*, *202*, 125–141. https://doi.org/10.1016/j.isprsjprs.2023.05.028

Zhou, Y., Smith, S. J., Elvidge, C. D., Zhao, K., Thomson, A., & Imhoff, M. (2014). A cluster-based method to map urban area from DMSP/OLS nightlights. *Remote Sensing of Environment*, *147*, 173–185. https://doi.org/10.1016/j.rse.2014.03.004